

# Determination of flow front velocity and optimal injection pressures for better impregnation of E-glass with polyester in resin transfer mold

Phaneendra Kumar KOPPARTHI<sup>\*.1</sup>, Vengal Rao KUNDAVARAPU<sup>2</sup>,  
Venkata Ravishankar DASARI<sup>3</sup>, Bhaskara Rao PATHAKOKILA<sup>1</sup>

\*Corresponding author

<sup>\*.1</sup>Department of Mechanical Engineering,  
Vignan's Lara Institute of Technology & Science,  
Vadlamudi, Andhra Pradesh, PIN. 522 213, India,  
phani\_vec@rediffmail.com\*, bhaskarengg153@gmail.com

<sup>2</sup>Department of Mechanical Engineering,  
Vignan's Foundation for Science, Technology and Research,  
Vadlamudi, Andhra Pradesh, PIN. 522 213, India,  
vengalrao.k@gmail.com

<sup>3</sup>Department of Mechanical Engineering,  
T.K.R College of Engineering & Technology, Hyderabad,  
Telangana, PIN. 500 079, India,  
shankardasari@rediffmail.com

DOI: 10.13111/2066-8201.2019.11.3.8

Received: 09 July 2019/ Accepted: 06 August 2019/ Published: September 2019

Copyright © 2019. Published by INCAS. This is an "open access" article under the CC BY-NC-ND license (<http://creativecommons.org/licenses/by-nc-nd/4.0/>)

**Abstract:** Flow front velocity of resin plays a key role in yielding better impregnation of fiber reinforcement in resin transfer molding to fabricate quality composites. A video camera was used to capture the patterns of resin flowing below the grid lines drawn on the acrylic sheet of resin transfer mold and also to accurately measure the flow front velocity using an image conversion tool. The effect of flow front velocity, permeability, Reynolds number and void content at five different injection pressures on chopped strand E-glass/polyester composites consisting of 4, 5 and 6 layers has been studied. On the basis of Reynolds number of resin flow and void content present in the composite, optimal injection pressures are suggested for better impregnation of preform. Composites processed at these injection pressures gave superior properties in tension and flexure. Fractured parts of the specimens were examined on Scanning Electron Microscope to explain the causes of superior mechanical properties.

**Key Words:** Flow front velocity, Reynolds number, void content, optimal pressure, permeability

## 1. INTRODUCTION

The use of glass fiber reinforced composites has been increasing in various applications such as aerospace, military, transport and other industries [1] due to improved mechanical properties than those of metals, of which properties are primarily dependent on their manufacturing process, reinforcement type, percentage of usage, size and shape [2, 3].

However in recent years, as the machining operations are reduced, a greater importance is given to the type of manufacturing quality composite products [4]. Coming to the manufacturing process, resin transfer molding proves to have great potential in the composite industry because it allows the production of structural parts with high fiber volume content in greater volumes at relatively low costs. Resin transfer molding (RTM) allows low fiber volume fraction and it can be enhanced by incorporating denser preform and increasing the injection pressure of resin. The increase of resin injection pressure not only results in mold deformation but also leads to fiber washout from the mold [5]. These consequences are eliminated by closing the mold during the resin transfer [6]. Richardson et al. [7] used an RTM for flow visualization of J2027L phenolic resin mixed with catalyst and allowed the resin mixture into the mold. Yulu Ma et al. [8] employed a rectangular mold with pressure pot system for injecting vinyl ester resin into randomly distributed glass fiber mat. Mathieu et al. [9] used an L-shaped mold with pressurized bucket for pumping resin into glass fiber mats and arranged point sensors to determine the displacement of resin flow. Bickerton et al. [10] used a mold with stiffening bars for avoiding deflections in the mold. But the bars became hindrance to estimate the flow front velocity of resin. In fact, flow front velocity, permeability, fiber volume fraction, void content, Reynolds number and injection pressure are dependent on the type of reinforcement, number of layers, arrangement of fiber in the mold and viscosity of the resin [11]. Moreover, the injection pressure of the resin plays a crucial role in the impregnation of fibers and flow front velocity [12] which ultimately effects the filling time. The flow front progression increases with increase in injection pressure when the resin injection occurs [13]. Therefore, one has to control the resin injection pressure for better impregnation of mold in order to minimize the content of voids under low and high resin velocities [14]. In the experiments conducted recently, images of test fluid were taken at equal intervals to monitor the flow front and treated with Matlab image processing code to calculate the flow front velocity [15]. The application of pressure transducers [16] and dielectric sensors [17] to flow monitoring in RTM gives normally local pressure values. However, the dielectric sensors could fail to detect the pressure of working fluid due to lack of impregnation, gelation and resin flow stop. The implementation of such devices to cover large cavity areas is complex and expensive.

To the authors' knowledge, many investigators have focused on the flow visualization study of resin and reported on low impregnation of reinforcement with resin due to the arrangement of multiple resin ports, stiffened bars and pressure sensors in the literature. Very few investigators have developed resin transfer molds with resin inlets at the center. Hence, an attempt has been done to overcome the above issues for visualizing the pattern of resin during impregnation in the customized RTM with central resin inlet under different injection pressures and also for determining the flow front velocities of resin accurately. Specifically, optimal injection pressures are reported based on the Reynolds number of resin flow for study of better mechanical properties of composites.

## 2. EXPERIMENTAL

### 2.1 Customized resin transfer mold

A customized resin transfer mold was manufactured for present investigations and its schematic diagram indicating all parts is shown in Fig. 1. The air from the foot-operated pump flows through the hose pipe, the air valve and enters the cylindrical resin tank at desirable pressure. A pressure gauge of 0.98 MPa capacity with 0.0196 MPa least count was

installed on a 3-liter capacity cylindrical resin tank to read the pressure of a resin flowing into the mold through the flow control valve.

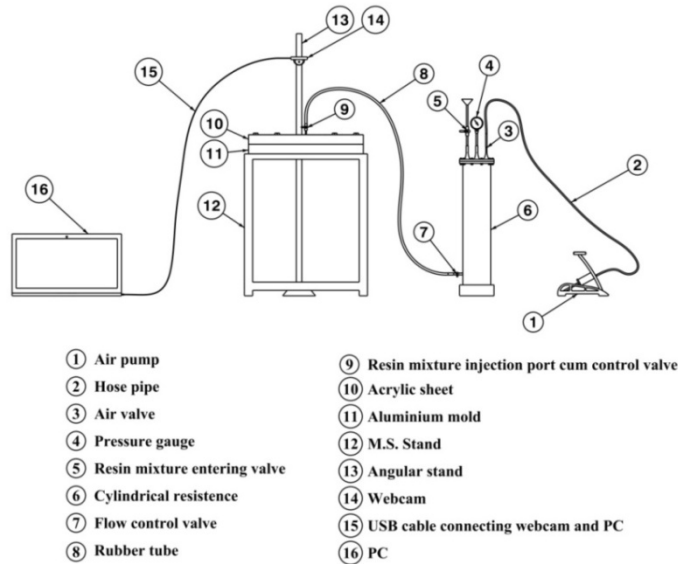


Fig. 1 - Schematic diagram of customized resin transfer mold

The resin tank has at its interior another pressure gauge of same capacity to indicate the pressure developed in the resin mixture. Once the tank is filled with certain quantity of resin mixture, it is closed with a tight valve applying sealant. The pressurized resin mixture released by the flow control valve flows through the rubber tube and exits from the injection port. The resin mixture entering valve, cylindrical resin tank, flow control valve and rubber tube were periodically cleaned for each experiment using pressurized D-13 NC thinner. The deflection of the mold alters the form of resin flow pattern hence to reduce it, mold was supported on clamps at the end faces.

## 2.2 Materials and laminates

The reinforcing and matrix materials of composites investigated are E-glass chopped strand fiber mat of 450 gsm (Code: M6450-104) and polyester resin (Viscosity:  $450 \pm 50$  Cp), respectively. Accelerator (Cobalt Naphthenate: 1.0%) and catalyst (Methyl Ethyl Ketone Peroxide: 1.25%) were used to prepare composites in customized RTM.

Three preforms, each consisting of 4, 5 and 6 layers of E-glass fiber mat were used to produce three laminates with 32.13 %, 40.94 % and 53.27 % volume fractions of fiber respectively.

Fiber volume fractions were determined as suggested by Chensong Dong [18]. The thickness of each laminate is 5 mm. All laminates were manufactured at various injection pressures of  $P_1 (= 0.196 \text{ MPa})$ ,  $P_2 (= 0.245 \text{ MPa})$ ,  $P_3 (= 0.294 \text{ MPa})$ ,  $P_4 (= 0.343 \text{ MPa})$  and  $P_5 (= 0.392 \text{ MPa})$ .

## 2.3 Flow front velocity, permeability, Reynolds number and void content

A typical pattern of resin flowing below the grid lines from center of the mold is shown in Fig. 2. The pressurized resin mixture flows through the injection port located at the center of mold. The resin mixture moves in a radial direction and impregnates into reinforcement.

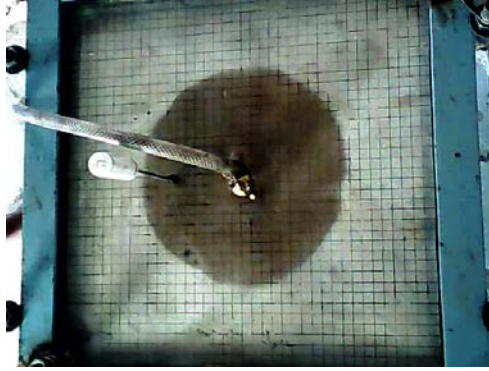


Fig. 2 - Typical pattern of resin flow

The pattern of resin flow below the grid lines drawn on an acrylic sheet of RTM was observed through a 2 Megapixel video camera located above the mold and its size was measured from minor and major gridlines drawn with adjacent gaps of 1 mm and 10 mm on acrylic sheet.

Flow front progression was recorded and digitized by the image conversion tool. Every digitized frame represents the resin flow traveled in one second to describe the flow front velocity.

As the quality of composites manufactured by RTM primarily depends on preform permeability, it was determined in the present work using Eq. (1) proposed by Bryan et al. [19].

$$K = \frac{Q\eta}{AP} \ln \left[ \frac{r_f}{r_i} \right] r_f \quad (1)$$

where,  $Q$  = volumetric flow rate,  $\eta$  = viscosity of resin,  $A$  = cross sectional area of the preform,  $P$  = resin injection pressure,  $r_i$  = size of the initial injection radius and  $r_f$  = size of radial flow front

$$\text{Size of the radial flow front, } r_f = \sqrt{\frac{Q}{\varepsilon \cdot \pi \cdot H} t + r_i^2} \quad (2)$$

where  $t$  = filling time,  $H$  = cavity height of the mold and  $\varepsilon$  = porosity

The porosity,  $\varepsilon$  is the percentage of pores inside preform and is given [5] by

$$\varepsilon = 1 - \frac{NA_w}{\rho_f T_m} \quad (3)$$

where  $N$  = number of plies,  $A_w$  = total weight of fabric ply,  $\rho_f$  = fiber density and  $T_m$  = thickness of the laminated fabric.

To predict the type of resin flow pattern in RTM process, Reynolds number [20] was calculated using Eq. (4) given below.

$$R_e = \frac{\rho_r U d_p}{\mu(1-\varepsilon)} \quad (4)$$

$\rho_r$  = resin density,  $U$  = velocity of resin,  $d_p$  = length of flow and  $\mu$  = dynamic viscosity of resin.

Based on the Reynolds number, the flow can be characterized as laminar for  $R_e < 10$ , transitional for  $10 < R_e < 300$  and turbulent for  $R_e > 300$ . Void formation reduces material

durability and makes it more susceptible to environmental conditions and moisture absorption. Hence, the void content should be minimized as much as possible. To know the void content present in the composites of current investigations, the test method B was adopted to determine the volume percentage of voids as per ASTM D2734-94 standards and the expression for void content is given by

$$V = 100 - M_d \left( \frac{w_r}{\rho_r} + \frac{w_f}{\rho_f} \right) \quad (5)$$

$M_d$  = measured density,  $w_r$  = weight of resin,  $w_f$  = weight of glass fiber,  $\rho_r$  = resin density and  $\rho_f$  = fiber density.

## 2.4 Testing of composites

Samples conforming to the shapes of ASTM D638 type-1 and D790 were separated from laminates for performing tensile and flexural tests.

Tensile tests were conducted on universal testing machine (UTM) of 100 kN capacity with a crosshead speed of 2 mm/min. Three-point-bend tests were also run on the same machine to determine the flexural strength of the composite.

The center distance between the supporting rollers is 100 mm. The rollers and mandrel placed on the specimen have the same diameter of 6 mm.

All tests were conducted at room temperature. No sample fractured at the grips. The complete physical separation of the material was noticed as failure of the specimen in both static and flexural tests with audible sound. Five specimens were tested and their average was considered to define both tensile and flexural strengths.

## 3. RESULTS AND DISCUSSIONS

The plots shown in Fig. 3 represent the flow front velocity plotted against the resin injection pressure for 4, 5 and 6 layered composites. The flow front velocity increases with resin injection pressure and decreases with increasing number of layers. Flow front velocity exhibited similar trend with resin injection pressure as reported by Jean et al. [21]. At constant fiber volume fraction, the mold filling time decreased with increasing resin injection pressure. Flow front velocity for composites processed at same injection pressure decreased with increasing number of layers due to increase in mold filling time. This can be stated by the fact that increased fiber volume fraction reduced the volumes of pore spaces in the preform. Hence, the resin flew at slower rate to wet the fiber.

The variation of Reynolds number with resin injection pressure is shown in Fig. 4. Flow regions of resin were classified into transition (for  $Re < 300$ ) and turbulent (for  $Re > 300$ ) [22]. Hence, in Fig. 4, a line has been drawn to demarcate both transition and turbulent regions. Reynolds number of resin flow enhanced with increasing injection pressure and decreased with increasing number of fiber layers. For composites at constant injection pressure, Reynolds number decreased due to decreasing flow front velocity. The Reynolds numbers of resin flow for composites manufactured at injection pressures  $P_1$  and  $P_2$  were less than 300 hence the flow was in transition zone. Of the three laminates molded under injection pressure  $P_3$ , the resin flow in 4 layered composite during impregnation was turbulent. For 4 and 5 layered molds, the resin flow through preform was turbulent at injection pressure  $P_4$ . It is interesting to note that the high injection pressure  $P_5$  resulted in erratic flow pattern for composites of the three different volume fractions.

From Fig. 5, the percent of voids present in the composites processed at the five different injection pressures can be noted. The percentage of voids in the composite decreased with increasing fiber volume fraction under same injection pressure due to formation of uniform flow fronts through small pore spaces of the fiber. However, lowest void volume fractions of 1.75 % at  $P_2$ , 1.54 % at  $P_3$  and 1.46 % at  $P_4$  were noticed in 4, 5 and 6 layered composites respectively due to better impregnation of fiber. At other pressures, the void content was increased. These voids produce stress concentrations in the composites during loading.

In the present study, composites processed with the customized RTM at injection pressures  $P_2$  (= 0.245 MPa),  $P_3$  (= 0.294 MPa) and  $P_4$  (= 0.343 MPa) had their resin flow patterns in transition zone and resulted better impregnation with minimum number of voids. Hence, the pressures  $P_2$ ,  $P_3$  and  $P_4$  were considered as optimal injection pressures. The number of voids in the laminates increased beyond their optimal injection pressures as the resin flow entered in to turbulent. Similar trend of voids formation was also reported by Chang et al. [23] after certain injection pressure.

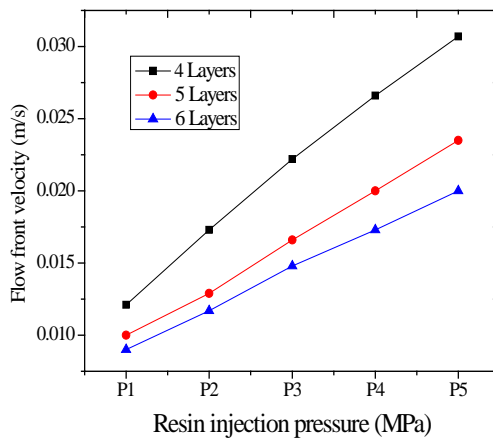


Fig. 3 - Comparison of flow front velocity with resin injection pressure

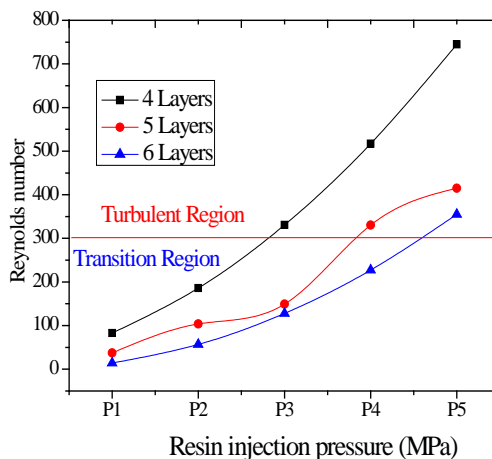


Fig. 4 - Reynolds number plotted with resin injection pressure

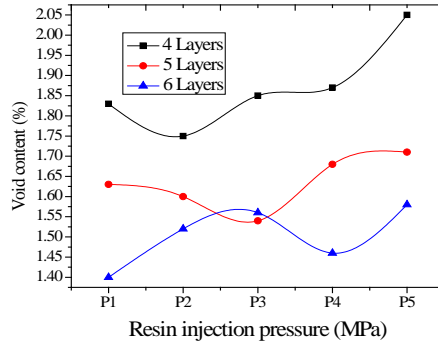


Fig. 5 - Variation of void content against resin injection pressure

Fig. 6 represents the variation of tensile strength with resin injection pressure. The tensile strength has increased with increasing volume fraction of fiber for composites molded under the same injection pressure. The authors noticed the increase of tensile strengths for the three composites processed under different pressures considered up to their respective optimal values due to decreasing number of voids formed as a result of better impregnation of fiber. Beyond the optimal injection pressures, strengths of composites began decreasing. The reason could be the displacement of fiber from the original position and formation of more voids. Maximum tensile strengths of 104.16 MPa, 126.81 MPa and 153.06 MPa were noticed for 4, 5 and 6 layered composites at their corresponding optimal injection pressures from Fig. 6. The authors understand that the maximum tensile strength of 153.06 MPa was achieved for 6 layered composites fabricated at flow front velocity of 0.017 m/s and optimal injection pressure of  $P_4$  ( $= 0.343$  MPa). Typical load displacement plots for laminates molded at their corresponding optimal injection pressures are shown in Fig. 7. The plots signify that the modulus increases with increase of fiber volume fraction. It can be inferred from the tensile strengths and Young's module presented in Table 1 for optimal resin injection pressures that six layered laminate had greater tensile strength compared to 4 and 5 layered composites. Patel et al. [24] reported a reduction of tensile strength for glass fiber/polyester composite from 21.8 MPa to 19.7 MPa when resin injection pressure increased from 30 psi to 60 psi as the investigators of this work noticed decrease of tensile strength for glass fiber/polyester composites beyond optimal injection pressure,  $P_4$  from 153.06 MPa to 136.7 MPa.

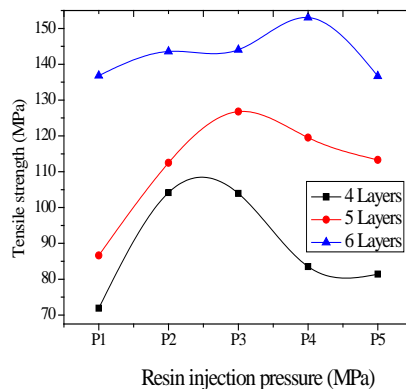


Fig. 6 - Variation of tensile strength with resin injection pressure

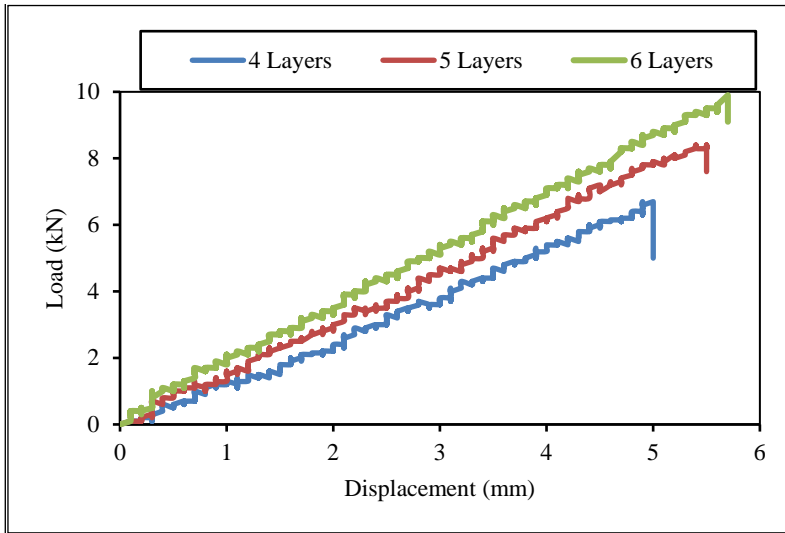


Fig. 7 - Load deflection plots at optimal injection pressures

Table 1. Mechanical properties of 4, 5 and 6 layered composites at optimal resin injection pressures

Specimen type	Optimal injection pressure (MPa)	Tensile strength (MPa)	Standard deviation	Young's modulus (GPa)	Standard deviation
4 layered	0.245	104.16	3.49	2.16	0.10
5 layered	0.294	126.81	4.23	2.51	0.24
6 layered	0.343	153.06	4.79	2.71	0.26

Data plotted in Fig. 8 represent the curves of flexural strength with resin injection pressure and also indicates the enhancement of flexural strength with increasing fiber volume fraction at the same injection pressure.

Composites of 4, 5 and 6 layers processed at optimal injection pressures performed in flexure with similar behavior in tension giving maximum flexural strengths of 87.36 MPa, 120.73 MPa and 151.23 MPa respectively.

Beyond these pressures, the flexural strength began decreasing due to increase of void content present in the composite as noticed by Karbhari et al. [25].

For 6 layered composite, the maximum flexural strength is 151.23 MPa at flow front velocity of 0.017 m/s and optimal injection pressure of  $P_4 (= 0.343 \text{ MPa})$ .

For the present glass fiber/polyester composites, the authors observed a reduction of flexural strengths beyond the optimal injection pressures (Fig. 8) when injection pressure increased to  $P_5$  as reported by Chang et al. [23] for the reduction of flexural strength of glass/epoxy composite from 584.7 MPa to 508.8 MPa when the resin injection pressure increased from 392 kPa to 490 kPa.

Fig. 9 indicates the variation of permeability plotted against the resin injection pressure. The permeability has decreased with increase in fiber volume fraction as remarked by Stadtfeld et al. [26].

The permeability of preforms increased at the same injection pressure. At optimal injection pressures, the composites had permeabilities of  $0.00016 \text{ m}^2$ ,  $0.00013 \text{ m}^2$  and  $0.00012 \text{ m}^2$  corresponding to the composite samples of 4, 5 and 6 layers.

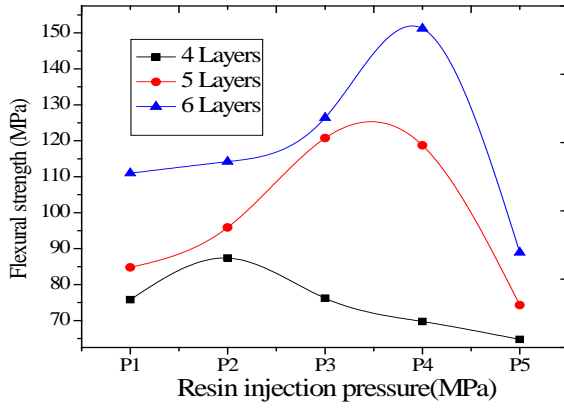


Fig. 8 - Variation of flexural strength with resin injection pressure

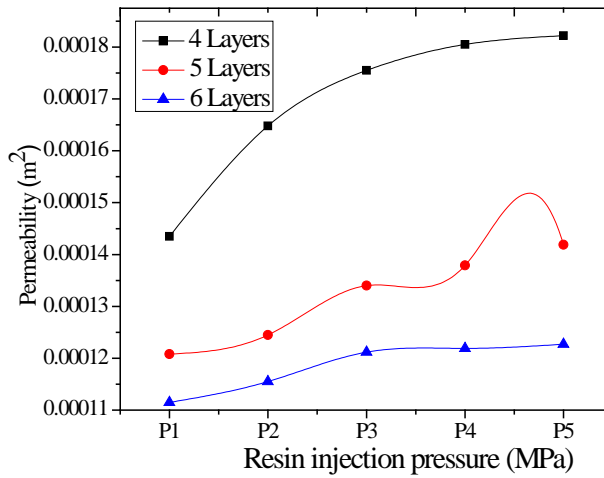
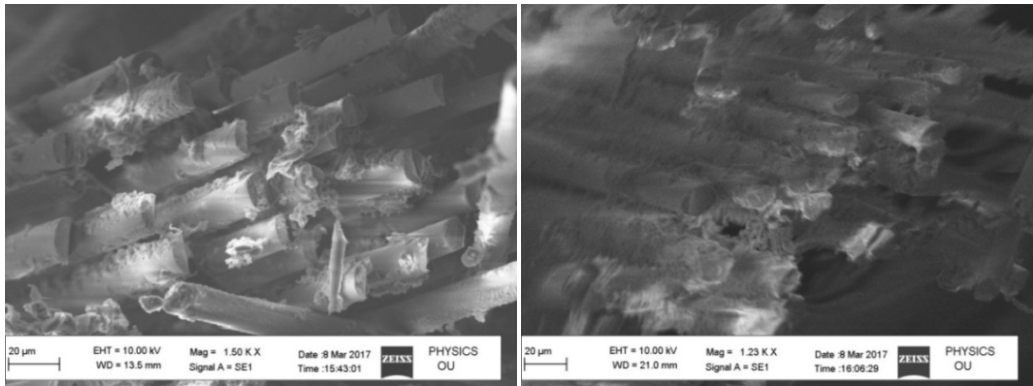
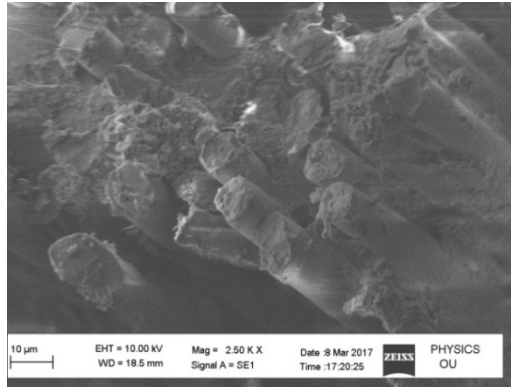


Fig. 9 - Variation of permeability with resin injection pressure



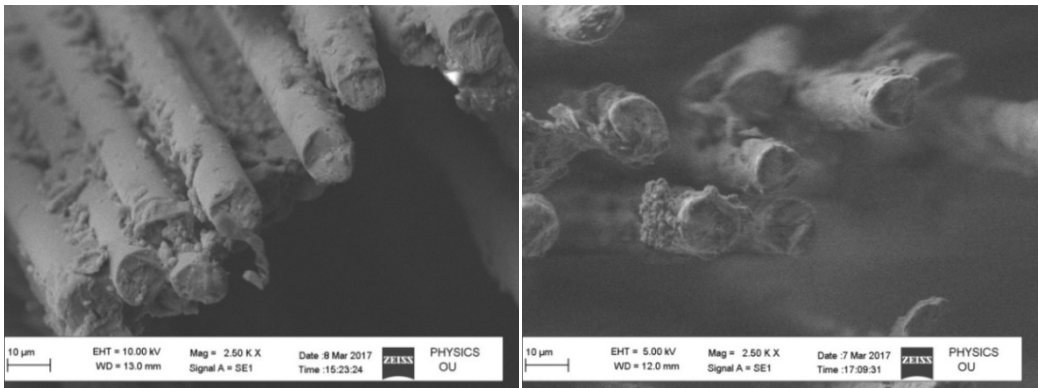
(a)

(b)



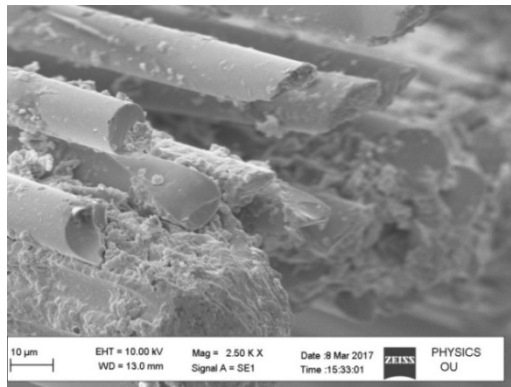
(c)

Fig. 10 - SEM images of samples tested in tension (a) 4 layers at P<sub>2</sub> (b) 5 layers at P<sub>3</sub> and (c) 6 layers at P<sub>4</sub>



(a)

(b)



(c)

Fig. 11 - SEM images of samples tested in flexure (a) 4 layers at P<sub>2</sub> (b) 5 layers at P<sub>3</sub> and (c) 6 layers at P<sub>4</sub>

SEM images of fractured surfaces of tensile and flexural test samples manufactured at optimal injection pressures are shown in Figs. 10 and 11. The composites with low fiber volume fractions had more debondings at various locations. Better adherence of fiber with matrix can be another reason for the maximum tensile and flexural strengths exhibited by 6 layered composite processed at pressure P<sub>4</sub> in addition to less void content present in it as viewed in Figs.10c and 11c. The fiber pullout of chopped strand fiber had cleared surface

without adhered resin as viewed by Volkan et al. [27] in SEM images, hence the fiber matrix adhesion was good for the processed composites.

#### 4. CONCLUSIONS

The customized RTM used in this work was successfully employed to fabricate good quality of E-glass/polyester composites with 4, 5 and 6 layers at various injection pressures of resin. In this study, the flow pattern was observed through video camera to record flow front progression and digitized using image conversion tool. Reynolds number was determined based on flow front velocity and the resin flow patterns were demarcated into transition and turbulent regions.

Optimal injection pressures  $P_2$ ,  $P_3$  and  $P_4$  were suggested based on the type of flow pattern of resin and percent of void content in the molded composites. At these pressures, better impregnation of fiber occurred in composites. Therefore, superior tensile and flexural strengths were obtained. Six layered composite fabricated at optimal injection pressure  $P_4$  ( $= 0.343$  MPa) had maximum tensile and flexural strengths.

#### REFERENCES

- [1] S. A. Hussain, V. Pandurangadu, K. P. Kumar, V. V. Bharath, A predictive model for surface roughness in turning glass fiber reinforced plastics by carbide tool (K-20) using soft computing, *Jordan Journal of Mechanical and Industrial Engineering*, **5**, pp. 433-438, 2011.
- [2] M. Ali, Synthesis and characterization of epoxy matrix composites reinforced with various ratios of TiC, *Jordan Journal of Mechanical and Industrial Engineering*, **10**, pp. 231-237, 2016.
- [3] A. M. Al-Huneidei, I. S. Jalham, Studying the properties of polymer blends sheets for decorative purposes, *Jordan Journal of Mechanical and Industrial Engineering*, **7**, pp.41-48, 2013.
- [4] M. R. Vinayaga, N. Rajeswari, S. K. Bala, Optimization studies on thrust force and torque during drilling of natural fiber reinforced sandwich composites, *Jordan Journal of Mechanical and Industrial Engineering*, **8**, pp. 385-392, 2014.
- [5] G. Hossein, Physical determination of permeability variation with porosity for composite preforms, *International Journal of Engineering Science, Industrial and Mechanical Engineering*, **18** (34), pp. 67-73, 2007.
- [6] C. D. Rudd, K. N. Kendall, Towards a manufacturing technology for high volume production of composite components, *Proceedings of Institution of Mechanical Engineers, Part B. Journal of Engineering Manufacture*, **206**, pp.77-91, 1992.
- [7] M. O. W. Richardson, Z. Y. Zhang, Experimental investigation and flow visualization of the resin transfer mould filling process for non-woven hemp reinforced phenolic composites, *Journal of Composites, Part A*, **31**, pp. 1303-1310, 2000.
- [8] M. Yulu, B. H. Xiao, W. U. Dongdi, The permeability of glass fiber mat and its influence on the filling time of RTM process, *Journal of Composites Processing and Microstructure*, pp. 19-26, 1997.
- [9] D. Mathieu, H. Kuang-Ting, G. Ali, S. G. Advani, On-line characterization of bulk permeability and race-tracking during the filling stage in resin transfer molding process, *Journal of Composite Materials*, **37** (17), pp. 1525-1541, 2003.
- [10] S. Bickerton, E. M. Sozer, P. J. Graham, S. G. Advani, Fabric structure and mold curvature effects on preform permeability and mold filling in the RTM process part I experiments, *Journal of Composites, Part A*, **31**, pp.423-438, 2000.
- [11] D. Mylene, B. Christophe, K. Patricia, Solution to filling time prediction issues for constant pressure driven injection in RTM, *Journal of Composites, Part A*, **36**, pp. 339-344, 2005.
- [12] D. Salvatori, B. Caglar, H. Teixeira, V. Michaud, Permeability and capillary effects in a channel-wise non-crimp fabric, *Journal of Composites, Part A*, DOI:10.1016/j.compositesa, 2018.02.015.
- [13] B. Thatiane, Y. H. Marcos, O. H. C. Maria, C. V. H. Jacobus, F. A. Caporalli, Experimental RTM manufacturing analysis of carbon/epoxy composites for aerospace application: non-crimp and woven fabric differences, *Journal of Materials Research*, **16**(5), pp. 1175-1182, 2013.

- [14] C. D. Fratta, G. Koutsoukis, F. Klunker, P. Ermanni, Fast method to monitor the flow front and control injection parameters in resin transfer molding using pressure sensors, *AIP Conference Proceedings*, DOI:10.1063/1.5016789, 2017.
- [15] E. Ameri, G. Lebrun, L. Laperriere, In-plane permeability characterization of a uni-directional flax/paper reinforcement for liquid composite molding processes, *Journal of Composites, Part A*, **85**, 52, 2016.
- [16] E. M. Sozer, P. Simacek, S. G. Advani, Resin transfer molding (RTM) in polymer matrix composites In *Manufacturing Techniques for Polymer Matrix Composites (PMCs)*, 1<sup>st</sup> ed., S. Advani, K. T. Hsiao, Eds., Cambridge, UK: *Woodhead Publishing Limited*, pp. 245-309, 2012.
- [17] P. Carlone, F. Rubino, V. Paradiso, F. Tucci, Multi-scale modeling and online monitoring of resin flow through dual-scale textiles in liquid composite molding processes, *Journal of Advance Manufacturing Technology*, DOI: 10.1007/s00170-018-1703-9, 2018.
- [18] C. Dong, Experimental investigations on the fiber preform deformation due to mold closure for composites processing, *International Journal of Advance Manufacturing Technology*, **71**, pp. 585, 2014.
- [19] L. M. Bryan, D. F. Claudio, D. D. M. Mario, M. Paoloermanni, Improving time effective and robust techniques for measuring in-plane permeability of fiber preform for LCM processing, *32<sup>nd</sup> International Conference Seico 11 Paris New Material Characteristics to Cover New Application Needs*, **201**(3A), pp. 204-211, 2011.
- [20] J. B. Matthew, *CFD simulation of flow through packed beds using the finite volume technique*, Ph.D Thesis, University of Exeter, Exeter. 2011.
- [21] S. L. Jean, R. Edu, Porosity reduction using optimized flow velocity in resin transfer molding, *Journal of Composites, Part A*, **39**, pp. 1859-1868, 2008.
- [22] I. Ziolkowska, D. Ziolkowski, Fluid flow inside packed beds, *Chemical Engineering Process*, **23**, pp. 137-164, 1988.
- [23] L. L. Chang, H. W. Kung, Resin transfer molding (RTM) process of a high-performance epoxy resin II: effects of process variables on the physical, static and dynamic mechanical behavior, *Journal of Polymer Engineering and Science*, **4**, pp. 935-943, 2000.
- [24] N. Patel, V. Rohatgi, L. J. Lee, Influence of processing and material variables on resin fiber interface in liquid composite molding, *Polymer Composites*, **14**(2), pp. 161-172, 1993.
- [25] V. M. Karbhari, S. G. Slotee, D. A. Steen Kamer, D. J. Wilkins, Effect of material process and equipment variables on the performance of resin transfer moulded parts, *Journal of Composite Manufacturing*, **3**, pp. 143, 1992.
- [26] H. C. Stadtfeld, M. Erninger, S. Bickerton, S. G. Advani, An experimental method to continuously measure permeability of fiber preforms as a function of fiber volume fraction, *Journal of Reinforced Plastics and Composites*, **21**, pp. 879-897, 2002.
- [27] C. Volkan, S. Mehmet, Experimental characterization of traditional composites manufactured by vacuum-assisted resin-transfer molding, *Journal of Applied Polymer Science*, **107**, pp. 1822-1830, 2008.